Low Temperature Physics/Fizika Nizkikh Temperatur, 2018, v. 44, No. 10, pp. 1278–1283

Convective heat transport in two-phase superfluid/vapor ^{4}He system

P. Urban, P. Hanzelka, and I. Vlček

The Czech Academy of Sciences, Institute of Scientific Instruments, 147 Královopolská, Brno, Czech Republic

D. Schmoranzer and L. Skrbek

Faculty of Mathematics and Physics, Charles University, 3 Ke Karlovu, Prague 121 16, Czech Republic
E-mail: skrbek@fzu.cz

Received April 24, 2018, published online August 28, 2018

We have recently shown that under certain cryogenic conditions heat can flow from a colder but constantly heated body to a hotter but constantly cooled body. Specifically, we have provided experimental evidence that heat flows through normal liquid and gaseous phases of ^{4}He from the constantly heated, but cooler, bottom plate of a Rayleigh–Bénard convection cell to its hotter, but constantly cooled, top plate. Here we report results of a modified experiment, where the bottom normal liquid helium layer is replaced by superfluid ^{4}He, providing, together with a superfluid film covering the entire cell interior, an effective thermal short-circuit. Applied heat input of order 1 W to the bottom plate results in simultaneous heating of the entire cell: this physical process can be viewed, at least approximately, as a series of subsequent equilibrium states, until upon reaching the superfluid transition the non-equilibrium processes described in our previous study [*Proc. Nat. Acad. Sci. USA* **110**, 8036 (2013)] are fully recovered.

Keywords: thermal convection, two-fluid heat, transport, superfluid ^{4}He.

1. Introduction

The low-temperature phases of both isotopes of helium [1,2] can be used as outstanding working fluids in controlled laboratory experiments in broadly defined fluid dynamics. This is still true even if limiting ourselves to the common isotope ^{4}He. Its normal liquid phase, historically called He I, represents a classical viscous Navier–Stokes fluid possessing a kinematic viscosity of order $v \simeq 10^{-4}$ cm^2/s, depending slightly on temperature and pressure [3], the lowest of all known common classical fluids. Together with the cryogenic ^{4}He gas (whose flow properties are well known [4] and can experimentally be tuned easily by changing temperature and pressure), they serve as very useful classical viscous working fluids, offering themselves as unique media for classical fluid dynamics with continuously tuneable properties suitable for generating flows not only with high Reynolds [5] and Rayleigh numbers [6], but also huge ranges of these flow parameters.

When cooled below the $T_\lambda \simeq 2.17$ K, He I undergoes a second-order superfluid phase transition; the low-temperature phase is known as He II. The physical properties of He II [1,2] cannot be described by classical physics; it is a quantum fluid displaying a number of extraordinary physical properties such as superfluidity and two-fluid behavior. In the context of this article it is important to point out that heat conductivity of He II (convective in nature) is extraordinarily high, more that six orders of magnitude higher than that of He I, and that a thin film of high heat conductivity covers nearly all solid surfaces of the cryogenic vessel containing He II, as long as their temperature does not exceed T_λ.

1.1. Rayleigh–Bénard convection

Over the last decade, our group has been utilizing the favorable fluid properties of cryogenic helium gas in experimental studies of Rayleigh–Bénard convection [7], which serves as a very useful model for fundamental studies of buoyancy driven flows occurring on many length scales across the Universe. Rayleigh–Bénard convection occurs in a fluid layer confined between two laterally infinite, perfectly conducting plates heated from below in a gravitational field, and for an Oberbeck–Boussinesq fluid [7] it is fully characterized by the Rayleigh, Ra, and the Prandtl numbers, Pr. The convective heat transfer efficiency is described by the Nusselt number, via the Nu = Nu(Ra;Pr)

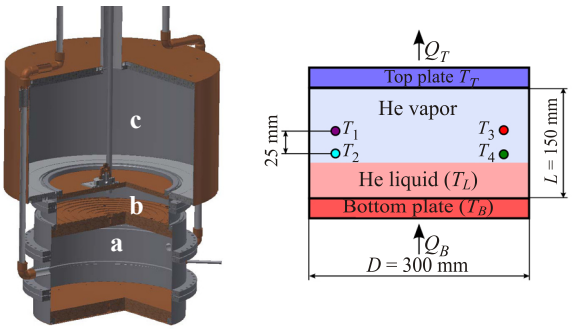

Fig. 1. (Color online) (Left) Three-dimensional view of the cryogenic insert of our Rayleigh–Bénard convection apparatus. The cylindrical Rayleigh–Bénard cell (a) in the bottom is thermally attached, via a heat exchange chamber (b) to the liquid helium vessel (c) above it. This cryogenic insert is placed in high vacuum inside a radiation shield thermally anchored to the liquid helium vessel (c). (Right) A schematic of the Rayleigh–Bénard cell heated from below and cooled from above, showing the placement of four small Ge sensors in its interior.

dependence. The principal dimensionless numbers describing Rayleigh–Bénard convection are defined as follows:

$$\mathrm{Nu} = \frac{LH}{\lambda \Delta T}; \quad \mathrm{Ra} = g\frac{\alpha}{v\kappa}\Delta T L^3; \quad \mathrm{Pr} = \frac{v}{\kappa}. \qquad (1)$$

Here H is the total convective heat flux density, g stands for the acceleration due to gravity, and ΔT is the temperature difference between the top and the bottom parallel plates separated by the vertical distance L. The properties of the working fluid are characterized by the thermal conductivity, λ, and by the ratio $\alpha/(v\kappa)$, where α is the isobaric thermal expansion, v is the kinematic viscosity, and κ denotes the thermal diffusivity.

In order to perform this research, we have designed and constructed a complex apparatus [8]. Its cryogenic insert is schematically shown in Fig. 1. With various modifications of the convection cell, this apparatus led to an important insight to high Ra turbulent Rayleigh–Bénard convection, relevant in particular to the possible existence of the phenomenologically predicted [9] ultimate regime of convection [10–13].

1.2. Two-fluid convection

More recently, we modified the same apparatus in order to study two-fluid convection in a Rayleigh–Bénard cell, across two horizontal layers: liquid He I and cryogenic ^{4}He gas. Our experiments led to interesting results [14,15]. One of them, directly relevant to this work, can be briefly described as follows.

We started very near equilibrium conditions, with the cell filled one-half with normal liquid helium and one-half with helium vapor. The temperature of the cell was approximately that of the thermally connected liquid helium vessel above it, see Fig. 1, corresponding to a point on the equilibrium saturated vapor curve, calculated based on the continuously monitored value of pressure, P, in the cell. Then we started heating the bottom plate and, using built-in germanium thermometers, continuously monitored the temperatures T_B and T_T of the bottom and top copper plates, as well as the temperatures T_1–T_4 of four small Ge sensors [16] inside the cell. Sometimes one of these sensors was used to measure the temperature fluctuations. The temperature of the upper plate was not controlled, but affected by the weak thermal link to the liquid helium vessel above, see again Fig. 1. For an isolated system consisting of liquid and vapor in equilibrium, one would expect that slow heating would result in partial evaporation of the liquid and uniformly rising temperature of the entire system along the saturated vapor curve.

This, however, was not the case. Upon switching on the uniformly distributed bottom plate heater, the bottom plate temperature T_B rose quickly with respect to the temperature of the liquid, T_L. This overheating of the bottom plate relative to the liquid, which would take much longer to heat up, resulted in nucleate boiling on the surface of the plate. From this point on, all subsystems in the cell heated up gradually. Contrary to expectations based on liquid/vapor equilibrium, the vapor became the hottest subsystem and, soon, even the cooled top plate became hotter than the heated bottom one, resulting in an apparent inversion of the heat flow, which formally corresponds to negative Rayleigh numbers. This situation at first sight appeared to contradict the second law of thermodynamics, e.g., its Clausius' formulation [17]: "No process is possible whose sole result is the absorption of heat from a body of lower temperature to a body of higher temperature".

In order to understand how heat could be transferred from the heated but cooler bottom plate to the cooled but hotter top plate, we had to realize that we are dealing with a non-equilibrium and unsteady system. The supplied heat is partly spent as latent heat to evaporate the liquid and to heat up and pressurize the cell interior. The observed anomalous heat transfer lasts only until the liquid layer in the cell disappears and can be broadly explained by means of a phenomenological model that assumes that heat from the bottom plate is partly absorbed by the liquid layer above it and partly carried to the vapor phase directly, increasing its density and pressure. The latter is accomplished by means of vapor bubbles, created at surface defects of the bottom plate via nucleate boiling, which, according to the literature [18,19], should indeed occur at the heated bottom plate for the conditions of our experiment.

An interesting question therefore emerges: How will this observation be affected when the bottom layer, normal liquid He I is replaced by superfluid He II? With this motivation at hand, we decided to answer this question experimentally.

2. Experimental results

The experiment is based on the Rayleigh–Bénard convection apparatus described in detail in Ref. 8. This time we use an aspect ratio $\Gamma = D / L = 2$ experimental cell (see Fig. 1), with the twice shorter stainless steel vertical wall but the same top and bottom plates, made of 28 mm thick annealed oxygen-free high conductivity copper of very high thermal conductivity (at least 2 kW/(m·K) at 5 K). The design of the heaters, glued in the spiral grooves milled on the external sides of plates, ensures better than 1 mK temperature homogeneity of the internal side of plates. In the experiment, the liquid helium vessel is pumped down in order to provide a constant temperature heat bath well below the λ temperature. Four calibrated Lake Shore GR-200A-1500-1.4B Ge temperature sensors (5 mK absolute accuracy guaranteed by the manufacturer) are embedded in the center and near the edge of both Cu plates. Additional home-made calibration of the Ge temperature sensors allows us to measure the temperature difference ΔT between the plates with uncertainty up to 2 mK [8]. Four small Ge sensors [16] are installed in the cell interior, in pairs positioned opposite at the half height of the cell, 1.5 cm from the sidewall and 2.5 cm vertically apart, see Fig. 1, calibrated within ±1 mK accuracy against our primary Lake Shore GR-200A-1500-1.4B Ge temperature sensors built into the bottom and top Cu plates.

The results of one particular run of our experiment are illustrated in Fig. 2. The experimental protocol is very similar to that described in Ref. 14. We again start very near equilibrium conditions, this time with the Rayleigh–Bénard cell partly filled with a liquid layer of superfluid helium and the rest of it with helium vapor. The temperature of the bottom plate $T_B \cong 1.88$ K, with T_T and T_1–T_3 (T_4 was used to measure the temperature fluctuations in the vapor) only slightly higher, thanks to the thermal link, via the helium exchange chamber, with the pumped down liquid helium vessel above. For the first 580 s, the bottom heater is off–no heat except a negligibly small parasitic heat leak is applied to the cell. Upon switching on a small heat input of 124 mW, all monitored temperatures in the cell start to increase. The increase is somewhat faster if higher heat input $Q_B = 0.535$ W is applied at $t = 750$ s and, again, when $Q_B = 1.014$ W is applied at $t = 870$ s, then it slows down due to a steep increase of the heat capacity of He II around 2 K. It is important to notice that all the temperatures in the cell grow simultaneously together, being nearly the same as the saturated vapor curve temperature $T_{\rm sat}$ calculated based on the continuously measured pressure in the cell, P. It is only past 1275 s, when the substantially larger heat input $Q_B = 2.08$ W is switched on, that an appreciable difference between the monitored temperatures gradually appears, with T_B being by 6–7 mK higher than T_T.

Upon reaching the λ temperature, clearly marked by a spike in the T_B record, the superfluid to normal second-order transition occurs and the situation drastically changes. The origin of the peak is physical and can be understood due to the fact that the bottom plate would overheat significantly above the liquid temperature before the boiling sets in (after overcoming the nucleation barrier) and starts carrying the heat away more efficiently. Conduction/convection in normal liquid is much less efficient at carrying the heat away and a notable temperature discontinuity develops on the boundary [18,19]. The normal fluid layer no longer provides a thermal short-circuit as it was in the case of the superfluid layer, thanks to the extremely efficient effective heat conductivity of thermal counterflow in He II and evaporation from the entire inner surface of the cell thanks to the superfluid film flow.

From now on, we are in the regime described in detail for the aspect ratio $\Gamma = 1$ cell in Ref. 14. This regime is il-

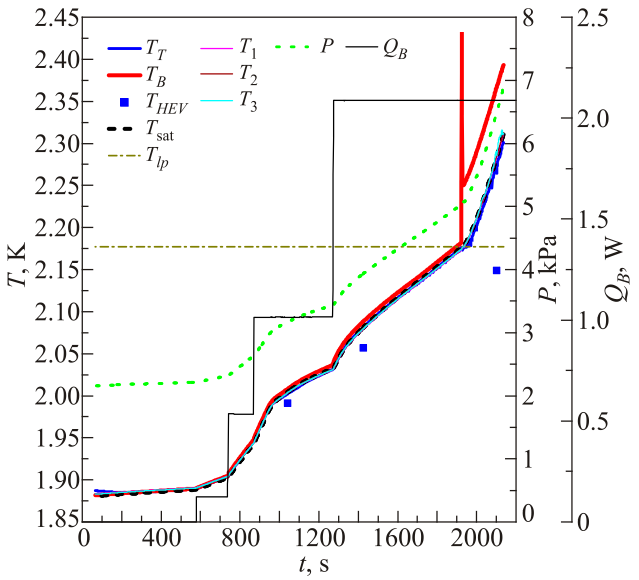

Fig. 2. (Color online) Two-phase superfluid/vapor ^{4}He experiment. Recorded time traces of pressure, P, in the cell and temperatures of the bottom plate, T_B, top plate, T_T, and of three small sensors (color-coded lines as indicated); T_1–T_3, all of them placed in the vapor. The blue solid squares denote the temperature of the pumped down helium vessel. The thick black broken line is the saturated temperature $T_{\rm sat}$ calculated from the measured pressure in the cell. The black solid line indicates the time and intensity of the heat input supplied by the heater to the bottom plate. The heat supplied to the bottom plate must be either stored in the system or leave through the top plate into the liquid helium vessel. Inside the cell, heat is exchanged between the two plates, liquid (including the superfluid film) and vapor, either by means of direct contact at interfaces, or via phase transition–evaporation/condensation at the liquid level, or condensation at the top plate. The horizontal dash/dot line indicates the λ temperature, where the second-order superfluid to normal phase transition occurs. It is clearly marked by a spike in the T_B temperature. From now on, the scenario repeats the observations reported in detail in our earlier work, Ref. 14.

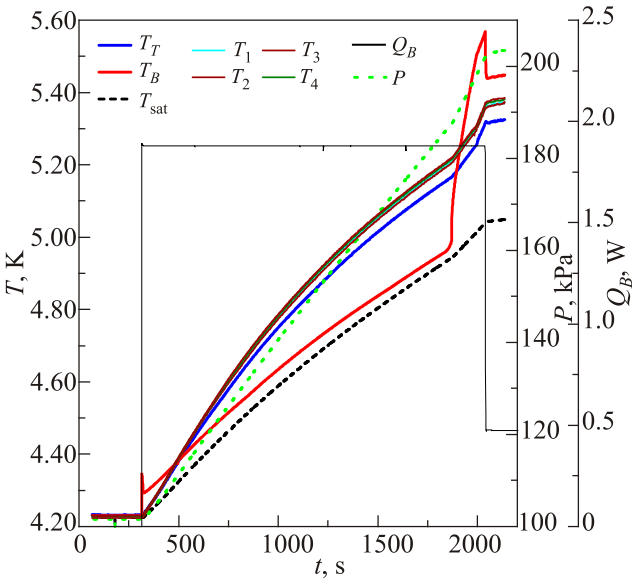

Fig. 3. (Color online) Two-phase normal liquid/vapor ^{4}He experiment. Recorded time traces of pressure, P, in the cell and temperatures of the bottom plate, T_B, top plate, T_T, and of four small sensors (color-coded lines as indicated); T_1–T_4, all placed in the vapor. All temperatures are nearly the same before switching on the bottom plate heater. The thick black broken line is again the saturated temperature T_{sat} calculated from the measured pressure in the cell. The black solid line indicates the time and intensity of the heat input supplied by the heater to the bottom plate. The scenario faithfully repeats the observations reported by us in Ref. 14, see the text for details.

lustrated for the aspect ratio $\Gamma = 2$ cell used in this experiment in Fig. 3. This experimental run starts with a relatively thin normal He I layer on the bottom plate, so that all temperature sensors T_1–T_4 are placed in the vapor. All measured temperatures in the cell are nearly the same before switching on the bottom plate heater delivering $Q_B = 1.9$ W, when the bottom plate temperature T_B rises quickly with respect to the temperature of the liquid. Note that the initial spike from extra overheating before boiling sets in is seen here, too. This overheating of the bottom plate relative to the liquid, which would take much longer to heat up, results in nucleate boiling on the surface of the plate. All subsystems in the cell heat up, the vapor gradually becomes the hottest subsystem and even the cooled top plate becomes hotter than the heated bottom one, resulting in an apparent inversion of the heat flow. In order to explain this extraordinary behavior, we developed a phenomenological model and numerically simulated this experiment reaching quantitative agreement between the theory and experiment [14]. This anomalous heat transport lasts only until the liquid He I layer becomes evaporated, which is marked by a steep increase in T_B, departing from the saturated vapor curve. Soon, the temperature distribution typical for Rayleigh–Bénard convection is established, characterized by the principal dimensionless numbers defined in Eq. (1), which depend on the heat supplied by the bottom plate heater.

3. Discussion

In order to fully understand the underlying physics of the two-fluid convection experiment which includes the superfluid liquid layer, it is useful to show its outcome in a slightly different way, see Fig. 4. All recorded traces of the temperature of the bottom plate, T_B, top plate, T_T, and of the three small sensors T_1–T_3 in the vapor are shown as a function of continuously monitored pressure P, i.e., in the coordinates of the PT phase diagram of ^{4}He. The time is just an implicit parameter here, but may be easily traced back using Fig. 2.

Figure 4 allows direct comparison of measured temperatures with that corresponding to the equilibrium saturated vapor curve. It clearly shows that below the λ temperature all recorded temperatures, on first approximation, agree with each other. This means that the time evolution of the states of the cell during an applied heat input of order 1 W to the bottom plate may be viewed, at least approximately, as a series of subsequent equilibrium states. As soon as the thermal short-circuit provided by the superfluid ^{4}He layer (we note that very low counterflow velocity of order

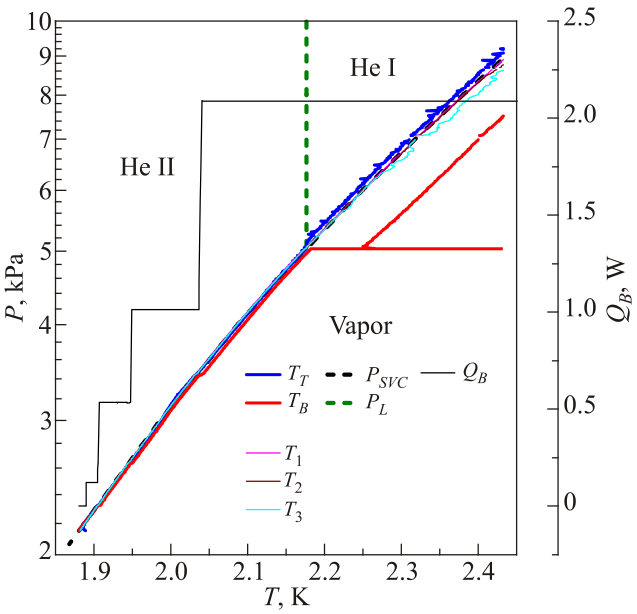

Fig. 4. (Color online) Recorded time traces of temperatures of the bottom plate, T_B, top plate, T_T, and of three small sensors (color-coded lines as indicated); T_1–T_3, placed in the vapor. Shown in the coordinates of the P–T phase diagram of ^{4}He; the data correspond one to one to Fig. 2. The black broken line is the equilibrium saturated vapor curve [3]. Time, here as an implicit parameter, progresses from the left to the right and may be traced back with the use of Fig. 2. The black solid line indicating the intensity of the heat input supplied by the heater to the bottom plate at the corresponding temperature. The λ point at the saturated vapor pressure curve is clearly marked by the departure of T_B from T_{sat}.

0.1 mm/s is sufficient to carry heat input of 1 W across the superfluid layer at temperatures around 2 K) and superfluid film is removed due to the superfluid to normal phase transition, we recover the more complex and highly interesting non-equilibrium situation (including detection of the rain of small helium droplets after switching off the bottom plate heater) described in detail in Ref. 14 and, from somewhat wider perspective, in the follow-up article by Niemela [15].

4. Conclusions

We have revisited our cryogenic two-fluid Rayleigh–Bénard convection experiment [14], using an aspect ratio $\Gamma = 2$ experimental cell, 30 cm in diameter. For similar experimental conditions, we confirm all results described in [14,15]. When, however, the bottom fluid layer — normal He I is replaced by superfluid He II which covers also the entire cell interior by a superfluid film and acts as a heat conduction short-circuit, we observe very different behavior. For heat inputs of order 1 W applied to the bottom plate all temperatures measured in the bottom and top plates and in the cell interior simultaneously grow and agree with each other as well as with the corresponding saturated vapor pressure temperature. This behavior holds until the superfluid to normal fluid transition is reached, above which the behavior observed in Ref. 14 is fully recovered.

Acknowledgments

The authors acknowledge technical help and fruitful discussions with M.J. Jackson, T. Králk, M. La Mantia, M. Macek, V. Musilová, K.R. Sreenivasan, A. Srnka and E. Varga. This research is funded by the Czech Science Foundation under project GAČR 17-03572S. IV acknowledges the support by MEYS CR project LO1212.

LS thanks Eduard Rudavskii, whom he first met as a young graduate student during the 6th Low Temperature School organized for Czech and Slovak physicists in May 1980 in Stará Lesná, Slovakia, and enjoyed his outstanding lectures introducing the extraordinary properties of superfluid helium, for long-lasting friendship and support of fruitful collaboration in the field of superfluidity between our low temperature laboratories. The authors wish him many more healthy and productive years in the research field of low temperature physics, to which he and his group have contributed so much.

1. V.M. Rizak, I.M. Rizak, and E.Ya. Rudavskii, *Kriogenna fizika i tekhnika*, Naukova Dumka, Kiev (2006).
2. D.R. Tilley and J. Tilley, *Superfluidity and Superconductivity*, Adam Hilger (1986).
3. R.J. Donnelly and C.F. Barenghi, *J. Phys. Chem. Ref. Data* **27**, 1217 (1998).
4. R.D. McCarty, *Thermophysical Properties of Helium-4 from 2 to 1500 K with Pressures to 1000 Atmospheres*, *Technical Note* **631**, National Bureau of Standards (1972); V.D. Arp and R.D. McCarty, *The Properties of Critical Helium Gas*, Tech. Rep., U. of Oregon (1998).
5. B. Saint-Michel, E. Herbert, J. Salort, C. Baudet, M. Bon Mardion, P. Bonnay, M. Bourgoin, B. Castaing, L. Chevillard, F. Daviaud, P. Diribarne, B. Dubrulle, Y. Gagne, M. Gibert, A. Girard, B. Hébral, Th. Lehner, B. Rousset, and SHREK Collaboration, *Phys. Fluids* **26**, 125109 (2014).
6. J.J. Niemela, L. Skrbek, K.R. Sreenivasan, and R.J. Donnelly, *Nature* **404**, 837 (2000).
7. F. Chillà and J. Schumacher, *Eur. Phys. J. E* **35**, 58 (2012).
8. P. Urban, P. Hanzelka, T. Kralik, V. Musilova, L. Skrbek, and A. Srnka, *Rev. Sci. Instrum.* **81**, 085103 (2010).
9. R.H. Kraichnan, *Phys. Fluids* **5**, 1374 (1962).
10. P. Urban, V. Musilová, and L. Skrbek, *Phys. Rev. Lett.* **107**, 014302 (2011).
11. P. Urban, P. Hanzelka, T. Kralik, V. Musilova, A. Srnka, and L. Skrbek, *Phys. Rev. Lett.* **109**, 154301 (2012).
12. P. Urban, P. Hanzelka, V. Musilova, T. Kralik, M. La Mantia, A. Srnka, and L. Skrbek, *New J. Phys.* **16**, 053042 (2014).
13. L. Skrbek and P. Urban, *J. Fluid Mech.* **785**, 270 (2015).
14. P. Urban, D. Schmoranzer, P. Hanzelka, K.R. Sreenivasan, and L. Skrbek, *Proc. Nat. Acad. Sci. USA* **110**, 8036 (2013).
15. J.J. Niemela, *Proc. Nat. Acad. Sci. USA* **110**, 7969 (2013).
16. Ge-on-GaAs *Film Sensors*, *TTR-G Model*, MicroSensor, Kiev, Ukraine.
17. R. Clausius, *Poggendorfs Annalen der Physik und Chemie* **79**, 368 and 500 (1850) [also in English: *Philos. Mag.* **2**, 1 and 102 (1851)].
18. R.V. Smith, *Cryogenics* **9**, 11 (1969).
19. S.W. VanSciver, *Helium Cryogenics*, *International Cryogenics Monograph Series*, Plenum Press, New York (1986).

Конвективне перенесення тепла в двофазній системі надплинна рідина/пар ^{4}He

P. Urban, P. Hanzelka, I. Vlček,
D. Schmoranzer, L. Skrbek

Нещодавно ми показали, що при певних кріогенних умовах тепло може надходити від тіла, яке є більш холодним, але постійно нагрівається, до тіла, яке є більш теплим, але постійно охолоджується. Зокрема, ми представили експериментальні дані, які свідчать про те, що тепло через нормальну рідку та газоподібну фази ^{4}He передається від більш холодної нижньої пластини комірки Релея–Бенара, яка постійно нагрівається, до більш гарячої верхньої пластині цієї комірки, яка постійно охолоджується. Наведено результати модифікованого експерименту, в якому шар рідкого гелію замінюється надплинним ^{4}He, що забезпечує, разом з надплинною поверхнею, що покриває всю внутрішню поверхню ко-

мірки, теплове коротке замикання. Прикладений тепловий потік близько 1 Вт на нижню пластину призводить до одночасного нагріву всієї комірки. Цей фізичний процес можна розглядати, принаймні приблизно, як ряд послідовних рівноважних станів, аж до досягнення надплинного переходу, нерівноважні процеси, які описані в нашому попередньому дослідженні [*Proc. Nat. Acad. Sci. USA* **110**, 8036 (2013)], повністю відновлені.

Ключові слова: теплова конвекція, дворідинний теплообмін, надплинний ^{4}He.

Конвективный перенос тепла в двухфазной системе сверхтекучая жидкость/пар ^{4}He

P. Urban, P. Hanzelka, I. Vlček,
D. Schmoranzer, L. Skrbek

Недавно мы показали, что при определенных криогенных условиях тепло может поступать от более холодного, но постоянно нагреваемого тела, к более горячему, но постоянно охлаждаемому телу. В частности, мы представили экспериментальные данные, свидетельствующие о том, что тепло через нормальную жидкую и газообразную фазы ^{4}He передается из постоянно нагреваемой, но более холодной нижней пластины конвективной ячейки Рэлея–Бенара, к более горячей, но постоянно охлаждаемой верхней пластине этой ячейки. Приведены результаты модифицированного эксперимента, в котором нижний нормальный слой жидкого гелия заменяется сверхтекучим ^{4}He, обеспечивая вместе со сверхтекучей поверхностью, покрывающей всю внутреннюю поверхность ячейки, тепловое короткое замыкание. Приложенный тепловой поток порядка 1 Вт на нижнюю пластину приводит к одновременному нагреву всей ячейки. Этот физический процесс можно рассматривать, по крайней мере приблизительно, как ряд последовательных равновесных состояний, вплоть до достижений сверхтекучего перехода, неравновесные процессы, описанные в нашем предыдущем исследовании [*Proc. Nat. Acad. Sci. USA* **110**, 8036 (2013)], полностью восстановлены.

Ключевые слова: тепловая конвекция, двухжидкостный теплообмен, сверхтекучий ^{4}He.